PLOS ONE

RESEARCH ARTICLE

Quantitative Analysis of Differential Proteome Expression in Bladder Cancer vs. Normal Bladder Cells Using SILAC Method

Ganglong Yang[1], Zhipeng Xu[2], Wei Lu[1], Xiang Li[3], Chengwen Sun[4], Jia Guo[1], Peng Xue[5]*, Feng Guan[1]*

1 The Key Laboratory of Carbohydrate Chemistry & Biotechnology, Ministry of Education, School of Biotechnology, Jiangnan University, Wuxi, China, **2** Shaanxi Provincial People's Hospital, Xi'an, China, **3** Wuxi Medical School, Jiangnan University, Wuxi, China, **4** Department of Urology, Affiliated Hospital of Jiangnan University, Wuxi, China, **5** Laboratory of Proteomics, Institute of Biophysics, Chinese Academy of Sciences, Beijing, China

* xuepeng@moon.ibp.ac.cn (PX); fengguan@jiangnan.edu.cn (FG)

Citation: Yang G, Xu Z, Lu W, Li X, Sun C, Guo J, et al. (2015) Quantitative Analysis of Differential Proteome Expression in Bladder Cancer vs. Normal Bladder Cells Using SILAC Method. PLoS ONE 10(7): e0134727. doi:10.1371/journal.pone.0134727

Editor: Jon M. Jacobs, Pacific Northwest National Laboratory, UNITED STATES

Received: January 20, 2015

Accepted: July 13, 2015

Published: July 31, 2015

Data Availability Statement: All relevant data are within the paper files and its Supporting Information files.

Funding: This work was supported by the National Science Foundation for Young Scientists of China (No. 81402115, 81201572), the Natural Science Foundation of Jiangsu Province, China (No. BK20140172) and the 111 Project of China (No.111-2-06). The funders had no role in study design, data collection and analysis, decision to publish, or preparation of the manuscript.

Abstract

The best way to increase patient survival rate is to identify patients who are likely to progress to muscle-invasive or metastatic disease upfront and treat them more aggressively. The human cell lines HCV29 (normal bladder epithelia), KK47 (low grade nonmuscle invasive bladder cancer, NMIBC), and YTS1 (metastatic bladder cancer) have been widely used in studies of molecular mechanisms and cell signaling during bladder cancer (BC) progression. However, little attention has been paid to global quantitative proteome analysis of these three cell lines. We labeled HCV29, KK47, and YTS1 cells by the SILAC method using three stable isotopes each of arginine and lysine. Labeled proteins were analyzed by 2D ultrahigh-resolution liquid chromatography LTQ Orbitrap mass spectrometry. Among 3721 unique identified and annotated proteins in KK47 and YTS1 cells, 36 were significantly upregulated and 74 were significantly downregulated with >95% confidence. Differential expression of these proteins was confirmed by western blotting, quantitative RT-PCR, and cell staining with specific antibodies. Gene ontology (GO) term and pathway analysis indicated that the differentially regulated proteins were involved in DNA replication and molecular transport, cell growth and proliferation, cellular movement, immune cell trafficking, and cell death and survival. These proteins and the advanced proteome techniques described here will be useful for further elucidation of molecular mechanisms in BC and other types of cancer.

Introduction

Bladder cancer (BC) is the fifth most common type of human cancer. There were an estimated 74,690 newly diagnosed cases and 15,580 deaths from this disease in the United States in 2013 [1]. Of total BC patients, >70% have nonmuscle-invasive disease and ~25% present initially with muscle invasion. Patients with the muscle-invasive form have a 50% risk of distant

Competing Interests: The authors have declared that no competing interests exist.

metastases and a poor prognosis [2]. The recurrence of superficial bladder tumors is a major reason for the worldwide prevalence of BC [3]. The majority (90%) of BCs are classified histologically as urothelial carcinomas (UCs), derived from the bladder urothelium [4]. Bladder epithelial tissues have a clear hierarchical organization consisting of three morphologically distinct cell types: basal, intermediate, and umbrella cells, corresponding respectively to early, middle, and late differentiation states [5]. Malignant transformation may occur in each of these cell types, resulting in a diversity of tumor phenotypes [6]. According to the latest report of the American Cancer Society, the relative 5-year survival rate for BC with early detection (stage I, (T1, N0, M0)) is ~88% [7]. Therefore, identification of novel early-stage molecular markers is desirable for improved risk stratification.

Candidate biomarkers for BC detection evaluated to date include telomerase, bladder tumor antigen (BTA), nuclear matrix protein 22 (NMP-22), and fibrin degradation product (FDP). The reliability of tests based on these biomarkers is poor because of low sensitivity and high false-positive rates [8–11]. Proteins can potentially be identified specific to aggressive or nonaggressive types of cancer. Proteome analysis is challenging because of the limited amount of available clinical sample [12]. Monitoring of the proteome of BC cells could provide additional information for clinical diagnostic purposes.

Recent advances in mass spectrometry (MS) for protein identification and quantification facilitate in-depth analysis of large numbers of proteins, and have been used for examination of the whole proteome in several systems. Such methods include 2D difference gel electrophoresis (2D DIGE), the similar iTRAQ (isobaric tag for relative and absolute quantitation), isotope-coded affinity tagging (ICAT), and stable isotope labeling by amino acids in cell culture (SILAC) [13–15]. In comparison with peptide-based absolute quantitation methods, SILAC has the advantages of mixing samples at the very beginning, and reduced sample-to-sample variability. Metabolic labeling with stable isotopes has been described as the "gold standard" in protein quantification [16]. Arginine (Arg) and lysine (Lys) are the stable isotope-labeled amino acids most frequently used in SILAC-based studies, because subsequent trypsin digestion of isolated proteins (which cleaves at basic residues) for MS analysis generates peptides with a single labeled amino acid, simplifying analysis and quantification [17]. In the present study, three stable isotopes each of Arg (R0, R6, R10) and Lys (K0, K4, K8)in three separate cultures ("light" (L), "medium" (M), and "heavy" (H)) were used to analyze proteome differences at various stages of BC. Distinctive L, M, and H forms of each peptide as detected by MS reflected relative amounts of the corresponding protein in three isotopically encoded BC cell stages.

Three human cell lines were studied: normal bladder epithelial HCV29, low grade nonmuscle invasive bladder cancer (NMIBC) KK47, and metastatic muscle invasive bladder cancer YTS1. Each of the three cell lines was cultured in media added with three combinations of unlabeled Lys and Arg ("light"), D_4-Lys and $^{13}C_6$-Arg ("medium"), and $^{13}C_6{}^{15}N_2$-Lys and $^{13}C_6{}^{15}N_4$-Arg ("heavy"). Proteins with >98% label incorporation were analyzed and quantified by 2D-HPLC-LTQ Orbitrap MS (Fig 1). Differential expression of the identified proteins, which

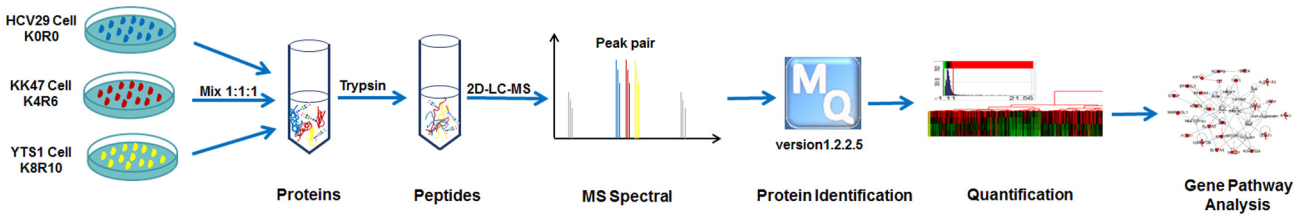

Fig 1. Schematic procedure for quantitative analysis of proteins in BC cells vs. normal bladder cells.

doi:10.1371/journal.pone.0134727.g001

are presumably related to BC development, was confirmed by western blotting, quantitative RT-PCR, and cell staining with specific antibodies.

Material and Methods

Cell culture

HCV29, KK47, and YTS1 cells were established as described previously [18–20] and kindly donated by Dr. Sen-itiroh Hakomori (The Biomembrane Institute; Seattle, WA, USA). Cells were cultured in RPMI 1640 medium supplemented with 10% FBS and 1% penicillin/ streptomycin at 37°C in 5% CO_2 atmosphere. For SILAC labeling, cells were cultured in SILAC-labeled RPMI 1640 with 10% dialyzed FBS and 1% penicillin/ streptomycin containing "light"(K0R0), "medium"(K4R6), or "heavy"(K8R10) Lys and Arg. To prevent Arg-to-Pro conversion, L-Pro (200 mg/L) was added to the medium as described previously [21]. Cells were cultured for at least 5 passages to eliminate nonlabeled Lys and Arg.

Cell lysis and protein extraction

Total proteins of the three cell lines were lysed and extracted using T-PER Reagent (Thermo Scientific; San Jose, CA, USA) according to the manufacturer's instruction. In brief, cells (~1×10^7) were detached with trypsin, washed twice with ice-cold 1×PBS (0.01 M phosphate buffer containing 0.15 M NaCl, pH 7.4), lysed with 1 mL T-PER reagent containing protease inhibitors (1 mM PMSF and 0.1% aprotinin), incubated for 30 min on ice, homogenized, and centrifuged at 12,000 rpm for 15 min. The supernatant was harvested and stored at -80°C. Protein concentration was determined by BCA assay (Beyotime; Haimen, China).

SDS-PAGE and *in-gel* digestion

Proteins were separated by 10% SDS-PAGE, visualized by Coomassie staining for 2 hr, and destained overnight. Excised gel slices were washed with 25 mM ammonium bicarbonate/ 50% acetonitrile (ACN). Dried pieces were incubated with 20 μL of 10 mM dithiothreitol (DTT) at 56°C for 1 hr and then with an equal volume of 20 mM iodoacetamide (IAM) at room temperature in the dark. Gel slices were washed and trypsinized with 20 μL (10 ng/μL) trypsin (Promega; Madison, WI, USA) for 30 min at 4°C. Excess trypsin solution was removed, 20 μL of 25 mM NH_4HCO_3 was added, and the mixture was incubated overnight at 37°C. Extracted products were dried with a SpeedVac concentrator (CentriVap Cold Trap, Labconco; Kansas, MO, USA) [22].

MALDI-TOF/TOF-MS

Dried samples were dissolved with 0.1% trifluoroacetic acid (TFA), spotted onto an MTP AnchorChip sample target, and air-dried. Peptides were recrystallized with matrix α-cyanohydroxycinnamic acid (CHCA; 1 μL of 10 mg/mL) and characterized by MALDI-TOF/TOF-MS (UltrafleXtreme, Bruker Daltonics; Bremen, Germany). Ionization was achieved by irradiation with a nitrogen laser (λ = 337 nm) operating at 20 Hz. Mass spectra were acquired using the FlexControl and FlexAnalysis software programs.

In-solution digestion

Proteins from three types of stable isotope-labeled cells were mixed at 1:1:1, reduced, and alkylated by incubation with equal amounts of 10 mM DTT and 20 mM IAM. Alkylated proteins were digested by trypsin added at a ratio of 1:50 (w/w) and incubated overnight at 37°C [23].

Total peptides were concentrated and desalted using a 10KD size-exclusion spin ultrafiltration unit and dried using a SpeedVac concentrator.

LC-MS/MS analysis

2D-LC-MS was performed using LTQ Orbitrap MS (Thermo Fisher Scientific; Waltham, MA, USA) as described previously [24]. Digested peptides (100 μg) were injected into a biphasic capillary column (i.d. 200 μm) packed with C_{18} resin (ReproSil-Pur, 5 μm, Dr. Maisch GmbH) and strong cation-exchange resin (Luna 5 μm SCX 100A, Phenomenex). Peptide effluents from the biphasic column at each step were directed into a 15-cm C_{18} analytical column (i.d. 75 μm, ReproSil-Pur, 3 μm) at flow rate 500 nl/min. Nano-ESI was performed with spray voltage 2.0 kV and heated capillary temperature 200°C. One full MS scan (300–1800) in the Orbitrap was followed by five MS/MS scans of the five most intense ions selected from the MS spectrum in LTQ. Charge state screening was enabled for +2, +3, +4, and above [25].

Data analysis

Raw MS data were analyzed using the MaxQuant software program (V. 1.2.2.5) [26,27]. A false discovery rate (FDR) of 0.01 for proteins and peptides and a minimum peptide length of 6 amino acids were required. MS/MS spectra were searched by Andromeda [28] against the IPI human database (V. 3.85). The MaxQuant program determined the SILAC state of peptides from mass differences between SILAC peptide pairs, and this information was used to perform searches with fixed Arg6 and Lys4 or Arg10 and Lys8 modifications, as appropriate. Quantification in MaxQuant was performed as described previously [26].

Differential regulation within each experimental M/L ("medium/ light") ratio and H/L ("heavy/ light") ratio of the identified proteins was normalized using z-score analysis, as described previously [29,30]. In brief, M/L and H/L ratios were converted into log2 space, and average ratios and SD (standard deviations) were calculated for each data set. The log2 M/L and H/L ratio of each protein were converted into a z-score, using the following formula:

$$\mathrm{z-scores}(\sigma) \quad \mathrm{of} \quad [\mathrm{b}] = \frac{\log_2 \frac{X(M \quad or \quad H)}{L}[b] - Average \quad of \quad (\log_2 of \quad each \quad number, \quad a \ldots n)}{Standard \quad deviation \quad of \quad (\log_2 of \quad each \quad number, \quad a \ldots n)}$$

where b were deemed as a single protein in a data set population (a. . ..n). The z-score was a measure of how many SD units (σ) of the log2 M/L or H/L ratio of the protein was away from the population mean. A z-score $\geq$1.960σ represented that differential expression of the protein lied outside the 95% confidence interval, a score $\geq$2.576σ represented expression outside the 99% confidence interval, and a score $\geq$3.291σ represented 99.9% confidence. Z-scores $\geq$1.960σ were considered to be significant [29].

Functional annotation and Ingenuity Pathways Analysis

Identified proteins were further analyzed using the SWISS-PROT database to classify their biological process, cellular component, and molecular function [31]. Significant over-represented gene ontology (GO) terms were identified using the Database for Annotation, Visualization and Integrated Discovery (DAVID) gene bioinformatic resources [32, 33]. Proteins determined to be differentially regulated as described in the preceding section were tabulated in Excel and their International Protein Index (IPI) numbers were uploaded into DAVID (http://david.abcc.ncifcrf.gov/home.jsp) for functional annotation analysis. Data sets containing gene identifiers and corresponding expression values were then uploaded into the Ingenuity Systems application. Each IPI

number was mapped to its corresponding gene object in the Ingenuity Pathways Knowledge Base. Networks of the proteins were generated algorithmically based on their connectivity. Fisher's exact test was used to calculate a p-value indicating the probability that a particular biological function and/or disease assigned to that network was due to chance alone.

Western blotting

Western blotting was performed as described previously [34]. In brief, proteins were separated on 10% SDS-PAGE gel, transferred onto a PVDF membrane, and the membrane was blocked using 5% nonfat milk in TBST and probed using specific antibodies. The primary antibodies were rabbit anti-insulin-like growth factor 2 mRNA-binding protein 1 (IGF2BP1) (#AP10466b, Abgent; San Diego, CA, USA), rabbit anti-melanoma-associated antigen 4 (MAGEA4) (#AP6166a, Abgent), rabbit anti-Thy-1 membrane glycoprotein (THY1) (#AP2050a, Abgent), 14-3-3 protein sigma (SFN) (#sc-365539, Santa Cruz Biotechnology, Dallas, TX, USA), rabbit anti-fibronectin (FN1) (#F3648, Sigma-Aldrich), mouse anti-vimentin (VIM) (#V5255, Sigma-Aldrich), CD70 antigen (CD70) (#sc-7681, Santa Cruz Biotechnology), and mouse anti-β-catenin (CTNNB1) (#610153, BD Biosciences; San Jose, CA, USA). The secondary antibodies were appropriate horseradish peroxidase (HRP)-conjugated rabbit anti-mouse or goat anti-rabbit (#A0216 and #A0208, Beyotime). Bands were visualized using an enhanced chemiluminescence detection kit (Westar Nova, Cyanagen; Bologna, Italy).

Quantitative real-time PCR

Cells (1×10^5 per well in a 6-well plate) were cultured and treated as described above. Total RNA was isolated using an RNApure Tissue Kit (CWBiotech; Beijing, China) according to the manufacturer's instructions. Primers were designed using the DNAMAN program (V. 6.0.3; Lynnon Biosoft, Canada). First-strand cDNA was synthesized from total RNA using ReverTra Ace-α (Toyobo; Osaka, Japan). Quantitative real-time PCR was performed by LightCycler-based SYBR Green I dye detection with UltraSYBR Mixture (CWBiotech). Gene expression was quantified by the $2^{-\Delta\Delta CT}$ method [35].

Cell staining

Cells were cultured on sterilized coverslips in 24-well plates until 70–80% confluence, washed, immobilized, permeabilized with 0.2% Triton X-100 for 10 min at room temperature, and blocked with 5% nonfat milk overnight at 4°C. Fixed cells were incubated with diluted primary antibodies for 12 hr, incubated with FITC-labeled secondary antibodies at 4°C for 6 hr in the dark, washed, stained with 4 μg/mL DAPI at room temp for 10 min, washed with 1×PBS, and photographed with a fluorescence microscope (Eclipse E600, Nikon; Tokyo, Japan).

Results

Determination of isotope incorporation efficiency

To analyze dynamic changes in BC oncogenesis at the proteome level, the SILAC method was applied to three bladder cell lines to obtain labeled cell populations. Sufficient labeling is a prerequisite for reliable quantification using this method. In the case of incomplete labeling of proteins, particularly for labeling efficiency <95%, quantitation of low-abundance proteins would be masked by contaminated "light" peptides. To determine incorporation efficiency of labeled Lys and Arg, "light" (HCV29), "medium" (KK47), and "heavy" (YTS1) proteins were separated, and the high-abundance protein was *in-gel* digested. MALDI-TOF/TOF-MS results for peptide GVVDSEDLPLNISR in heat shock protein 90 (P08238) indicated that complete

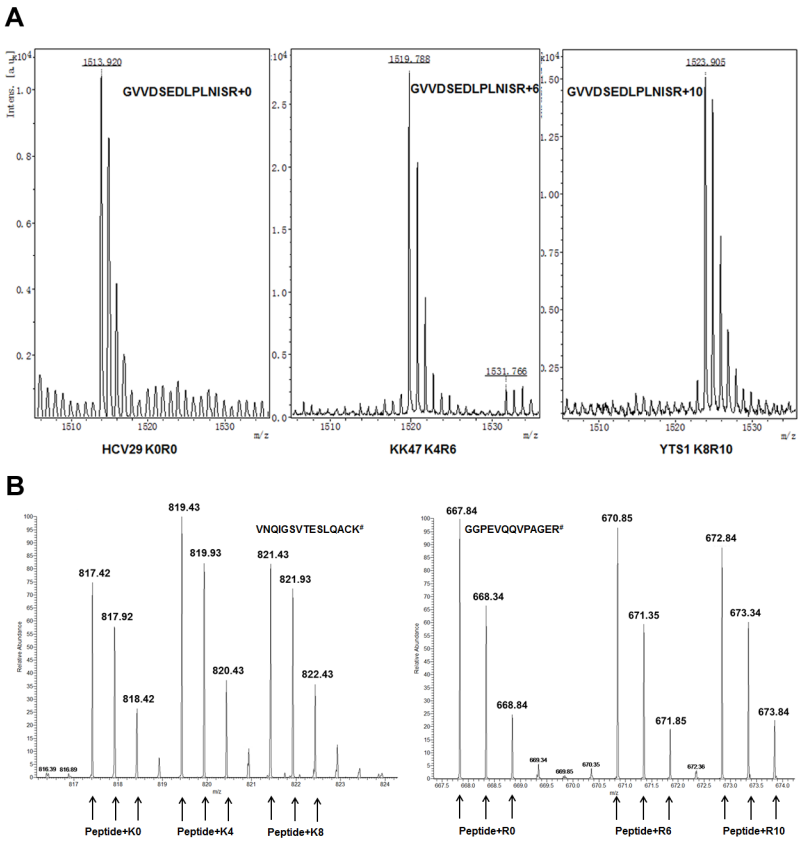

Fig 2. Mass spectrometric analysis of stable isotope-labeled proteins (SILAC method). (A) Determination of incorporation efficiency by MALDI-TOF/TOF-MS. Peaks annotated as R0 (left), R6 (middle), and R10 (right) are peptide GVVDSEDLPLNISR of heat shock protein 90 from HCV29, KK47, and YTS1 cells. (B) Identification and quantification of proteome in BC cells by 2D-HPLC LTQ Orbitrap MS. Peaks annotated as K0, K4, and K8 (left) and R0, R6, and R10 (right) are doubly charged peptide VNQIGSVTESLQACK of alpha enolase and GGPEVQQVPAGER of fatty acid synthase.

doi:10.1371/journal.pone.0134727.g002

incorporation of isotopically labeled Arg and Lys was achieved in KK47 and YTS1, and no Arg-to-Pro conversion occurred (Fig 2A). LC-ESI-MS/MS analysis of the doubly charged peptide VNQIGSVTESLQACK of alpha-enolase (P06733) and GGPEVQQVPAGER of fatty acid synthase (P49327) showed that these doublets of actual peak clusters were from HCV29, KK47, and YTS1 cells, respectively (Fig 2B).

SILAC cell model for quantification of proteome in BC progression

Proteins isolated from the three cell lines were mixed (1:1:1) and digested using a 10 KD filter (Millipore; Billerica, MA, USA). Peptides were analyzed by ultrahigh-resolution liquid chromatography-tandem MS (nLC-ESI-MS/MS) on a hybrid linear ion trap LTQ Orbitrap instrument. A total of 3721 unique proteins were identified in two independent replicate experiments (Fig 3A and S1 Table). Of these, 1766 proteins (47.5% of the total) that were identified in both experiments and satisfied the criteria established for protein quantitation were subjected to further bioinformatic analysis. The distribution histograms of log ratios for both M/L and H/L fit a Gaussian distribution. Most of the identified proteins were within the ±1 range of log ratios (Fig 3C and 3D). Using 1 as the threshold log ratio, expression of 255 proteins was higher in both KK47 and HCV29, and expression of 434 proteins was lower in both KK47 and HCV29

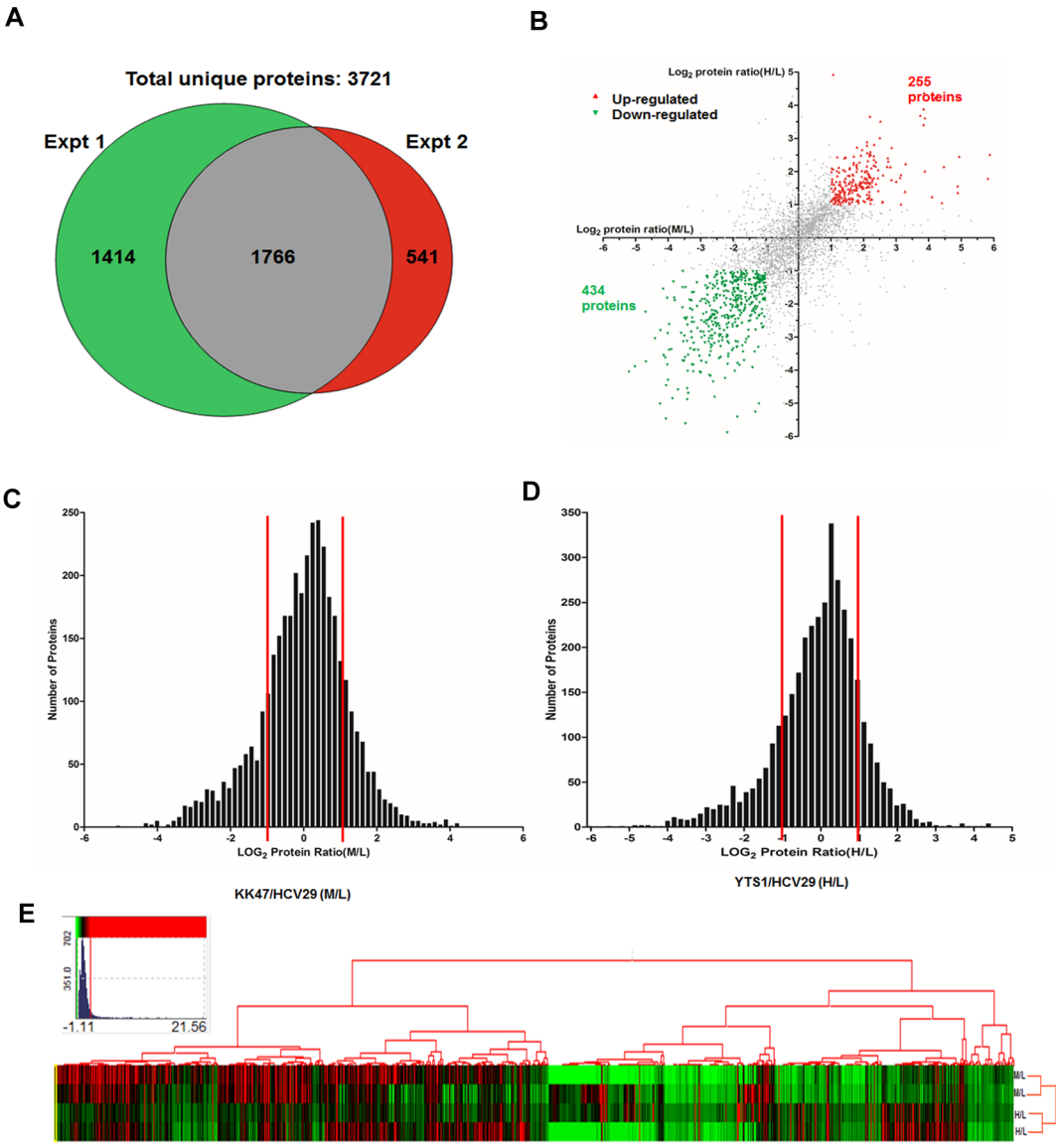

Fig 3. Distributions of proteins identified in various experiments described in the text. (A) Venn diagrams of numbers of identified proteins from individual experiments. (B) Ratios of KK47/HCV29 (M/L) and YTS1/HCV29 (H/L) for the set of 1766 proteins. log2 of the SILAC ratio for each protein (n = 2) reflects differences in relative expression among KK47, YTS1, and HCV29 cells. (C) Distribution of SILAC M/L ratios. (D) Distribution of SILAC H/L ratios. (E) Cluster graph ("heat map") generated by hierarchical clustering of significant regulated proteins after averaging z-scores using a 95% cutoff.

doi:10.1371/journal.pone.0134727.g003

(Fig 3B). Population distribution-based z-scores allowed direct comparison of proteins from different experiments. Differing confidence level cutoffs were applied to the data by z-score analysis to determine which proteins were significantly differentially regulated. The cutoffs applied were 95%, 99% and 99.9%, corresponding to z-scores of ±1.960, ±2.576, and ±3.291, respectively. Using a 95% cutoff, significant differential regulation was observed for 110 proteins in KK47 vs. HCV29 (36 upregulated, 74 downregulated) and for 87 proteins in YTS1 vs. HCV29 (17 up, 70 down). Differential regulation was observed for 35 proteins in the two BC lines vs. HCV29 using a 99% cutoff (2 up, 33 down), but for only five of these proteins using a 99.9% cutoff (2 up, 3 down) (Table 1). Tables 2 and 3 list the upregulated and downregulated proteins determined in the two experiments, with their average SILAC ratios and z-scores. All

Table 1. Protein number, log2 ratio mean±SD, and z-scores of SILAC-labeled proteins.

Cell line	Mean log 2	SD Log 2	z-scores[a]		
			±1.960σ	±2.576σ	±3.291σ
KK47 (M/L)	-0.072	1.237	36, 74	13, 22	7, 3
YTS1 (H/L)	-0.151	1.143	17, 70	6, 27	1, 3
Both cell lines			2, 33	2, 3	0, 0

[a]The first and second value shown are, respectively, the number of upregulated and downregulated proteins outside the indicated confidence level.

doi:10.1371/journal.pone.0134727.t001

proteins differentially regulated with >95% confidence had a >5-fold alteration of SILAC ratios, and most proteins differentially regulated with >99% confidence had a >10-fold alteration of SILAC ratios.

Hierarchical clustering analysis of samples was performed to examine correlations of proteome patterns among the three cell lines. The Cluster graph ("heat map") shows that samples of the same cell line cluster together (Fig 3E). Some proteomes were distinctive among the three cell lines based on significant alterations in metastatic vs. low grade nonmuscle invasive, whereas other proteomes were moderate and consistent. Proteins in the former group may be involved in BC development.

Functional classification and pathway analysis of identified proteins

Functional interpretation is a crucial step in data analysis when extensive functional annotation of the data sets is not available. Taking into account their nonexclusive localization in GO, the identified proteins were linked to at least one annotation term each within the GO molecular function, biological process, and molecular component categories. The most common molecular functions were binding (47.2%), and catalytic activity (30.9%) (Fig 4A). The major biological process categories were cellular (16.3%), single-organism (14.2%), and metabolic (13.8%) (Fig 4B). The major cellular component categories were cell (17.6%), cell part (17.6%), and organelle (15.8%) (Fig 4C).

To identify enrichment terms associated with the upregulated and downregulated groups of proteins after averaging of z-scores using the 95% cutoff, lists of proteins were uploaded to the DAVID website using the complete human proteome as background. To help clarify which molecular functions and biological processes were most affected during BC maturation, over-represented GO terms were identified based on threshold count ≥ 2 and Expression Analysis Systematic Explorer (EASE) < 0.1. The over-represented molecular functions, biological processes, and cellular components in the significant enriched GO terms of upregulated proteins were analyzed. The most highly ranked molecular function was neutral amino acid transmembrane transporter activity (2 proteins). The most highly ranked biological processes were cellular amino acid derivative metabolic process (4 proteins), ribonucleoprotein complex biogenesis (4 proteins), response to extracellular stimulus (4 proteins), and nitrogen compound biosynthetic process (4 proteins). The most highly ranked cellular components were intracellular non-membrane-bounded organelle (14 proteins) and non-membrane-bounded organelle (14 proteins).

Next, over-represented molecular functions, biological processes, and cellular components in the significant enriched GO terms of downregulated proteins were analyzed. The most highly ranked molecular functions were calcium ion binding (16 proteins), structural molecule activity (11 proteins), and identical protein binding (10 proteins). The most highly ranked biological processes were cell adhesion (14 proteins), biological adhesion (14 proteins), response

Table 2. Upregulated proteins in BC cells with >95% confidence[a].

Swiss-prot	Gene name	Protein name	M/L average	H/L average	log2 M/L average	log2 H/L average	z-scores M/L	z-scores H/L
C9JGI3_HUMAN	TYMP	Thymidine phosphorylase	39.51	1.43	5.30	0.51	4.35	0.47
FOLR1_HUMAN	FOLR1	Folate receptor alpha	31.73	2.91	4.99	1.54	4.09	1.30
J3QRJ3_HUMAN	THY1	Thy-1 membrane glycoprotein	29.72	2.57	4.89	1.36	4.01	1.16
RCN3_HUMAN	RCN3	Reticulocalbin-3	23.97	3.29	4.58	1.72	3.76	1.45
STEA4_HUMAN	STEAP4	Metalloreductase STEAP4	23.43	4.23	4.55	2.08	3.74	1.74
EF1A2_HUMAN	EEF1A2	Elongation factor 1-alpha 2	17.58	0.87	4.14	-0.20	3.40	-0.10
1433S_HUMAN	SFN	14-3-3 protein sigma	16.87	3.27	4.08	1.71	3.35	1.44
DDX21_HUMAN	DDX21	Nucleolar RNA helicase 2	14.33	10.65	3.84	3.41	3.16	2.82
KCRB_HUMAN	CKB	Creatine kinase B-type	14.15	1.30	3.82	0.38	3.15	0.37
CPSM_HUMAN	CPS1	Carbamoyl-phosphate synthase [ammonia], mitochondrial	12.22	0.99	3.61	-0.01	2.98	0.05
MTAP_HUMAN	MTAP	S-methyl-5-thioadenosine phosphorylase	11.66	10.09	3.54	3.33	2.92	2.75
ASSY_HUMAN	ASS1	Argininosuccinate synthase	11.08	1.86	3.47	0.89	2.86	0.78
H0YDA6_HUMAN	NAPRT1	Nicotinate phosphoribosyltransferase	10.23	2.82	3.35	1.49	2.77	1.27
1A68_HUMAN	HLA-A	HLA class I histocompatibility antigen, A-32 alpha chain	8.34	0.44	3.06	-1.19	2.53	-0.91
EPIPL_HUMAN	EPPK1	Epiplakin	8.12	0.86	3.02	-0.21	2.50	-0.11
PGH2_HUMAN	PTGS2	Prostaglandin G/H synthase 2	7.95	1.13	2.99	0.17	2.48	0.20
HPDL_HUMAN	HPDL	4-hydroxyphenylpyruvate dioxygenase-like protein	7.93	1.13	2.99	0.18	2.47	0.20
K1C18_HUMAN	KRT18	Keratin, type I cytoskeletal 18	7.51	2.18	2.91	1.13	2.41	0.97
WDR3_HUMAN	WDR3	WD repeat-containing protein 3	7.26	3.36	2.86	1.75	2.37	1.47
PADI2_HUMAN	PADI2	Protein-Arg deiminase type-2	6.99	1.38	2.81	0.46	2.33	0.43
EXOS4_HUMAN	EXOSC4	Exosome complex component RRP41	6.57	3.20	2.72	1.68	2.26	1.42
A6PVX1_HUMAN	SELENBP1	Selenium-binding protein 1	6.41	1.04	2.68	0.06	2.23	0.10
KYNU_HUMAN	KYNU	Kynureninase	6.32	0.35	2.66	-1.50	2.21	-1.16
4F2_HUMAN	SLC3A2	4F2 cell-surface antigen heavy chain	6.24	0.88	2.64	-0.18	2.19	-0.09
PO210_HUMAN	NUP210	Nuclear pore membrane glycoprotein 210	6.16	1.05	2.62	0.07	2.18	0.12
G3V588_HUMAN	ITPK1	Inositol-tetrakisphosphate 1-kinase	6.09	1.71	2.61	0.77	2.17	0.68
ANM7_HUMAN	PRMT7	Protein Arg N-methyltransferase 7	5.99	2.18	2.58	1.13	2.15	0.97
S100P_HUMAN	S100P	Protein S100-P	5.92	0.62	2.57	-0.69	2.13	-0.50
B0S8I7_HUMAN	LAGE3	L antigen family member 3	5.87	4.50	2.55	2.17	2.12	1.81
J3QKT4_HUMAN	PYCR1	Pyrroline-5-carboxylate reductase;	5.72	2.35	2.52	1.23	2.09	1.05
MCMBP_HUMAN	MCMBP	Mini-chromosome maintenance complex-binding protein	5.65	4.77	2.50	2.25	2.08	1.88
PRI2_HUMAN	PRIM2	DNA primase large subunit	5.47	4.59	2.45	2.20	2.04	1.84
K1C17_HUMAN	KRT17	Keratin, type I cytoskeletal 17	5.39	0.89	2.43	-0.16	2.02	-0.07
LAT1_HUMAN	SLC7A5	Large neutral amino acids transporter small subunit 1	5.35	1.27	2.42	0.34	2.01	0.34
MYPN_HUMAN	MYPN	Myopalladin	5.34	0.88	2.42	-0.19	2.01	-0.09
NPM3_HUMAN	NPM3	Nucleoplasmin-3	5.29	3.29	2.40	1.72	2.00	1.45
UHRF1_HUMAN	UHRF1	E3 ubiquitin-protein ligase UHRF1	4.98	5.13	2.32	2.36	1.93	1.97
ITA6_HUMAN	ITGA6	Integrin alpha-6	4.58	12.65	2.19	3.66	1.83	3.02
CND3_HUMAN	NCAPG	Condensin complex subunit 3	4.04	5.67	2.01	2.50	1.69	2.08
UBS3B_HUMAN	UBASH3B	Ubiquitin-associated and SH3 domain-containing protein B	3.88	6.30	1.96	2.66	1.64	2.21
E9PD53_HUMAN	SMC4	Structural maintenance of chromosomes protein	3.51	5.72	1.81	2.52	1.52	2.09

(*Continued*)

Table 2. (*Continued*)

Swiss-prot	Gene name	Protein name	M/L average	H/L average	log2 M/L average	log2 H/L average	z-scores M/L	z-scores H/L
KIF4A_HUMAN	KIF4A	Chromosome-associated kinesin KIF4A	3.26	6.56	1.70	2.71	1.44	2.25
MRP_HUMAN	MARCKSL1	MARCKS-related protein	2.74	5.39	1.45	2.43	1.23	2.02
CTRO_HUMAN	CIT	Citron Rho-interacting kinase	2.66	5.31	1.41	2.41	1.20	2.01
CIP2A_HUMAN	KIAA1524	Protein CIP2A	1.87	5.15	0.90	2.36	0.79	1.97
MAGA4_HUMAN	MAGEA4	Melanoma-associated antigen 4	1.48	17.47	0.56	4.13	0.51	3.40
PLEK2_HUMAN	PLEK2	Pleckstrin-2	0.98	5.95	-0.02	2.57	0.04	2.14
AL1A3_HUMAN	ALDH1A3	Aldehyde dehydrogenase family 1 member A3	0.93	13.75	-0.11	3.78	-0.03	3.12
RGS10_HUMAN	RGS10	Regulator of G-protein signaling 10	0.79	6.50	-0.34	2.70	-0.22	2.24
E41L3_HUMAN	EPB41L3	Band 4.1-like protein 3	0.72	6.54	-0.47	2.71	-0.33	2.25
UCHL1_HUMAN	UCHL1	Ubiquitin carboxyl-terminal hydrolase isozyme L1	0.42	9.45	-1.25	3.24	-0.95	2.68

[a]Proteins shown have at least one z-score value (M/L or H/L) $\geq$1.960σ in two biological replicates.

doi:10.1371/journal.pone.0134727.t002

to wounding (13 proteins), and immune response (13 proteins). The most highly ranked cellular components were plasma membrane (40 proteins), plasma membrane part (30 proteins), and non-membrane-bounded organelle (24 proteins) (S2 Table).

Proteins were further analyzed, and metabolic and canonical pathways and interconnecting proteins were generated, using Ingenuity Pathways Analysis (IngenuityH Systems, www.ingenuity.com). The top network functions identified as upregulated proteins in BC cells were involved in DNA replication, amino acid metabolism, molecular transport (52 proteins; Fig 5A), gene expression and hereditary disorders (33 proteins), cell growth and proliferation (20 proteins; Fig 5B), and post-translational modification and cancer (4 proteins). The top network functions identified as downregulated proteins in BC cells were cellular movement and immune cell trafficking (97 proteins; Fig 5C), lipid metabolism (31 proteins; Fig 5D), cellular development, growth and proliferation, and cell death and survival (6 proteins). These findings indicate that BC cell proteomes were continuously shifting depending on the stage of cell metastasis.

Confirmation of MS results by western blotting

Variations of the differential proteins described above were confirmed by western blotting. THY1, MAGEA4, IGF2BP1 and SFN were detected at higher levels in BC KK47 and YTS1 cells than in normal bladder epithelial HCV29 cells, whereas VIM, CTNNB1, FN1 and CD70 were detected at lower levels in KK47 and YTS1 than in HCV29 (Fig 6B and 6C). In general, the western blotting results were consistent with the variables from MS analysis (Fig 6A; S1 Table and S1 Fig).

Confirmation of SILAC results by qRT-PCR

The expression of six responding genes at the transcriptional level was evaluated by qRT-PCR. In BC KK47 and YTS1 cells, expression of *MAGEA4*, *THY1*, and *IGF2BP1* was significantly increased, whereas that of *VIM*, *CTNNB1*, and *FN1* was greatly reduced (Fig 6D). These findings are consistent with SILAC results.

Table 3. Downregulated proteins in BC cells with >95% confidence[a].

Swiss-prot	Gene name	Protein name	M/L average	H/L average	log2 M/L average	log2 H/L average	z-scores M/L	z-scores H/L
1C07_HUMAN	HLA-C	HLA class I histocompatibility antigen	0.17	0.02	-2.53	-6.05	-1.99	-4.83
A8MUB1_HUMAN	TUBA4A	Tubulin alpha-4A chain	0.35	0.09	-1.51	-3.42	-1.16	-2.70
AL1B1_HUMAN	ALDH1B1	Aldehyde dehydrogenase X, mitochondrial	0.11	0.10	-3.14	-3.34	-2.48	-2.64
ALDR_HUMAN	AKR1B1	Aldose reductase	0.11	0.04	-3.13	-4.58	-2.48	-3.65
ANO10_HUMAN	ANO10	Anoctamin-10	0.16	0.17	-2.65	-2.53	-2.09	-1.99
ARMC9_HUMAN	ARMC9	LisH domain-containing protein ARMC9	0.16	0.12	-2.67	-3.10	-2.10	-2.45
ASC_HUMAN	PYCARD	Apoptosis-associated speck-like protein containing a CARD	0.15	0.38	-2.72	-1.39	-2.14	-1.06
AT2B4_HUMAN	ATP2B4	Plasma membrane calcium-transporting ATPase 4	0.16	0.06	-2.65	-3.96	-2.08	-3.15
B2MG_HUMAN	B2M	Beta-2-microglobulin	0.42	0.10	-1.24	-3.29	-0.95	-2.60
BCAT1_HUMAN	BCAT1	Branched-chain-amino-acid aminotransferase, cytosolic	0.09	0.57	-3.41	-0.80	-2.70	-0.59
BIN1_HUMAN	BIN1	Myc box-dependent-interacting protein 1	0.21	0.12	-2.22	-3.09	-1.74	-2.44
CATB_HUMAN	CTSB	Cathepsin B	0.07	0.37	-3.84	-1.45	-3.05	-1.11
CAV1_HUMAN	CAV1	Caveolin-1;Caveolin	0.16	0.38	-2.68	-1.40	-2.11	-1.08
CBPA4_HUMAN	CPA4	Carboxypeptidase A4	0.11	0.08	-3.18	-3.73	-2.51	-2.96
CD70_HUMAN	CD70	CD70 antigen	0.16	0.10	-2.65	-3.26	-2.09	-2.58
CD97_HUMAN	CD97	CD97 antigen	1.98	0.17	0.99	-2.59	0.86	-2.04
CD99_HUMAN	CD99	CD99 antigen	0.14	0.82	-2.84	-0.28	-2.24	-0.17
CKAP4_HUMAN	CKAP4	Cytoskeleton-associated protein 4	0.16	0.23	-2.64	-2.12	-2.07	-1.66
CNN3_HUMAN	CNN3	Calponin-3	0.11	0.42	-3.25	-1.25	-2.57	-0.95
CO3_HUMAN	C3	Complement C3	0.84	0.15	-0.26	-2.77	-0.15	-2.18
CO6A2_HUMAN	COL6A2	Collagen alpha-2(VI) chain	0.07	0.26	-3.81	-1.96	-3.02	-1.52
CO6A3_HUMAN	COL6A3	Collagen alpha-3(VI) chain	0.12	0.17	-3.11	-2.56	-2.46	-2.01
CO7A1_HUMAN	COL7A1	Collagen alpha-1(VII) chain	0.34	0.10	-1.56	-3.39	-1.20	-2.68
COPZ2_HUMAN	COPZ2	Coatomer subunit zeta-2	0.06	0.02	-4.07	-5.47	-3.23	-4.37
CPPED_HUMAN	CPPED1	Calcineurin-like phosphoesterase domain-containing protein 1	0.10	0.11	-3.33	-3.15	-2.63	-2.49
D6RJ89_HUMAN	ACOX3	Peroxisomal acyl-coenzyme A oxidase 3	0.18	0.12	-2.44	-3.07	-1.92	-2.43
DCBD2_HUMAN	DCBLD2	Discoidin, CUB and LCCL domain-containing protein 2	0.29	0.16	-1.77	-2.68	-1.38	-2.11
DOP2_HUMAN	DOPEY2	Protein dopey-2	0.06	0.28	-4.03	-1.82	-3.20	-1.42
DPYL3_HUMAN	DPYSL3	Dihydropyrimidinase-related protein 3	0.10	0.40	-3.27	-1.31	-2.59	-1.00
E7EUD0_HUMAN	DKK3	Dickkopf-related protein 3	0.17	0.20	-2.57	-2.34	-2.02	-1.83
ES8L2_HUMAN	EPS8L2	Epidermal growth factor receptor kinase substrate 8-like protein 2	0.34	0.09	-1.56	-3.47	-1.20	-2.75
F5GY03_HUMAN	SPARC	SPARC	0.12	0.15	-3.01	-2.76	-2.38	-2.17
F8WCU2_HUMAN	FKBP7	Peptidyl-prolyl cis-trans isomerase	0.16	0.19	-2.67	-2.38	-2.10	-1.87
FA49A_HUMAN	FAM49A	Protein FAM49A	0.13	0.14	-2.96	-2.83	-2.34	-2.23
FHL1_HUMAN	FHL1	Four and a half LIM domains protein 1	0.13	0.09	-2.89	-3.55	-2.28	-2.81
FHL2_HUMAN	FHL2	Four and a half LIM domains protein 2	0.14	0.17	-2.88	-2.58	-2.27	-2.03
FINC_HUMAN	FN1	Fibronectin	0.11	0.13	-3.25	-2.96	-2.57	-2.33
FKB10_HUMAN	FKBP10	Peptidyl-prolyl cis-trans isomerase FKBP10	0.67	0.07	-0.57	-3.80	-0.40	-3.01
FLNC_HUMAN	FLNC	Filamin-C	0.17	2.65	-2.59	1.41	-2.03	1.19
FPRP_HUMAN	PTGFRN	Prostaglandin F2 receptor negative regulator	0.25	0.06	-1.99	-4.09	-1.55	-3.25

(*Continued*)

Table 3. (*Continued*)

Swiss-prot	Gene name	Protein name	M/L average	H/L average	log2 M/L average	log2 H/L average	z-scores M/L	z-scores H/L
FUCO_HUMAN	FUCA1	Tissue alpha-L-fucosidase	0.14	0.16	-2.82	-2.60	-2.22	-2.05
G3V2M6_HUMAN	STAT2	Signal transducer and activator of transcription 2	0.19	0.17	-2.41	-2.52	-1.89	-1.98
GABT_HUMAN	ABAT	4-aminobutyrate aminotransferase, mitochondrial	0.03	0.15	-5.07	-2.72	-4.04	-2.14
GBP1_HUMAN	GBP1	Interferon-induced guanylate-binding protein 1	0.12	0.13	-3.09	-2.93	-2.44	-2.31
GBP2_HUMAN	GBP2	Interferon-induced guanylate-binding protein 2	0.09	0.12	-3.46	-3.09	-2.74	-2.44
GELS_HUMAN	GSN	Gelsolin	0.11	0.25	-3.14	-1.99	-2.48	-1.55
GLSK_HUMAN	GLS	Glutaminase kidney isoform, mitochondrial	0.17	0.37	-2.53	-1.43	-1.99	-1.10
GPX1_HUMAN	GPX1	Glutathione peroxidase 1	0.74	0.11	-0.44	-3.14	-0.30	-2.48
H0Y8D1_HUMAN	PRSS1	Trypsin-1	0.05	0.06	-4.22	-4.01	-3.36	-3.18
H0YGX7_HUMAN	ARHGDIB	Rho GDP-dissociation inhibitor 2	0.09	1.91	-3.40	0.93	-2.69	0.81
H7C2T5_HUMAN	POFUT2	GDP-fucose protein O-fucosyltransferase 2	0.13	0.31	-2.91	-1.67	-2.30	-1.29
H7C5L1_HUMAN	PTGES2	Prostaglandin E synthase 2	1.46	0.12	0.55	-3.11	0.50	-2.46
HM13_HUMAN	HM13	Minor histocompatibility antigen H13	0.17	0.26	-2.52	-1.95	-1.98	-1.52
HYEP_HUMAN	EPHX1	Epoxide hydrolase 1	0.26	0.13	-1.93	-2.96	-1.50	-2.34
ICAM1_HUMAN	ICAM1	Intercellular adhesion molecule 1	0.58	0.13	-0.80	-2.91	-0.58	-2.30
ITA3_HUMAN	ITGA3	Integrin alpha-3	0.13	0.19	-2.90	-2.39	-2.29	-1.87
ITAV_HUMAN	ITGAV	Integrin alpha-V	0.12	0.13	-3.05	-2.90	-2.41	-2.29
ITPR3_HUMAN	ITPR3	Inositol 1,4,5-trisphosphate receptor type 3	0.30	0.11	-1.76	-3.15	-1.36	-2.49
JAM1_HUMAN	F11R	Junctional adhesion molecule A	0.06	0.08	-4.09	-3.63	-3.25	-2.87
K1C10_HUMAN	KRT10	Keratin, type I cytoskeletal 10	0.13	0.12	-2.95	-3.06	-2.33	-2.41
K1C9_HUMAN	KRT9	Keratin, type I cytoskeletal 9	0.13	0.09	-2.89	-3.49	-2.28	-2.76
K2C1_HUMAN	KRT1	Keratin, type II cytoskeletal 1	0.12	0.11	-3.07	-3.12	-2.42	-2.47
K7ENN8_HUMAN	TRIM16	Tripartite motif-containing protein 16	0.21	0.11	-2.22	-3.21	-1.74	-2.54
L1CAM_HUMAN	L1CAM	Neural cell adhesion molecule L1	0.43	0.10	-1.22	-3.33	-0.92	-2.63
LAMB1_HUMAN	LAMB1	Laminin subunit beta-1	0.16	1.20	-2.64	0.27	-2.08	0.27
LASP1_HUMAN	LASP1	LIM and SH3 domain protein 1	0.16	0.18	-2.69	-2.44	-2.12	-1.91
LEG3_HUMAN	LGALS3	Galectin-3	0.71	0.09	-0.49	-3.55	-0.34	-2.81
LRP1_HUMAN	LRP1	Prolow-density lipoprotein receptor-related protein 1	0.20	0.12	-2.33	-3.01	-1.83	-2.38
MAOX_HUMAN	ME1	NADP-dependent malic enzyme;Malic enzyme	0.31	0.11	-1.67	-3.23	-1.29	-2.55
MAP1B_HUMAN	MAP1B	Microtubule-associated protein 1B	0.09	0.24	-3.44	-2.09	-2.72	-1.63
MICA2_HUMAN	MICAL2	Protein-methionine sulfoxide oxidase MICAL2	0.18	0.26	-2.51	-1.95	-1.97	-1.52
ML12A_HUMAN	MYL12A	Myosin regulatory light chain 12A	0.09	0.19	-3.43	-2.41	-2.71	-1.89
MMP14_HUMAN	MMP14	Matrix metalloproteinase-14	0.10	0.27	-3.34	-1.88	-2.64	-1.46
MOT4_HUMAN	SLC16A3	Monocarboxylate transporter 4	0.72	0.06	-0.47	-4.00	-0.32	-3.17
MYH9_HUMAN	MYH9	Myosin-9	0.13	0.22	-2.97	-2.17	-2.34	-1.70
MYL9_HUMAN	MYL9	Myosin regulatory light polypeptide 9	0.11	0.16	-3.19	-2.67	-2.52	-2.10
NIBAN_HUMAN	FAM129A	Protein Niban	0.13	1.19	-2.94	0.25	-2.32	0.26
NMES1_HUMAN	NMES1	Normal mucosa of esophagus-specific gene 1 protein	0.40	0.06	-1.33	-3.95	-1.02	-3.14
NXP20_HUMAN	FAM114A1	Protein NOXP20	0.23	0.15	-2.14	-2.73	-1.68	-2.15

(*Continued*)

Table 3. (*Continued*)

Swiss-prot	Gene name	Protein name	M/L average	H/L average	log2 M/L average	log2 H/L average	z-scores M/L	z-scores H/L
OAS3_HUMAN	OAS3	2-5-oligoadenylate synthase 3	0.25	0.16	-2.02	-2.63	-1.58	-2.07
PAI2_HUMAN	SERPINB2	Plasminogen activator inhibitor 2	0.08	0.42	-3.64	-1.25	-2.88	-0.95
PDLI1_HUMAN	PDLIM1	PDZ and LIM domain protein 1	0.15	0.39	-2.76	-1.35	-2.18	-1.03
PEA15_HUMAN	PEA15	Astrocytic phosphoprotein PEA-15	0.15	0.37	-2.74	-1.43	-2.16	-1.10
PLSL_HUMAN	LCP1	Plastin-2	0.11	0.06	-3.20	-3.95	-2.53	-3.13
PML_HUMAN	PML	Protein PML	0.14	0.15	-2.79	-2.70	-2.20	-2.13
PNKD_HUMAN	PNKD	Probable hydrolase PNKD	0.18	0.14	-2.48	-2.84	-1.95	-2.24
PPGB_HUMAN	CTSA	Lysosomal protective protein	0.17	0.28	-2.58	-1.84	-2.03	-1.43
PTRF_HUMAN	PTRF	Polymerase I and transcript release factor	0.15	0.53	-2.74	-0.91	-2.16	-0.68
Q5RHS7_HUMAN	S100A2	Protein S100-A2	1.27	0.17	0.35	-2.59	0.34	-2.04
RAI14_HUMAN	RAI14	Ankycorbin	0.14	0.43	-2.87	-1.21	-2.26	-0.92
RCN1_HUMAN	RCN1	Reticulocalbin-1	0.46	0.16	-1.11	-2.67	-0.84	-2.10
RGPS2_HUMAN	RALGPS2	Ras-specific guanine nucleotide-releasing factor RalGPS2	0.10	0.40	-3.32	-1.32	-2.63	-1.01
S10A6_HUMAN	S100A6	Protein S100-A6	0.31	0.07	-1.71	-3.91	-1.32	-3.10
SAMH1_HUMAN	SAMHD1	SAM domain and HD domain-containing protein 1	0.35	0.11	-1.53	-3.21	-1.18	-2.54
SELM_HUMAN	SELM	Selenoprotein M	0.72	0.14	-0.48	-2.81	-0.33	-2.21
SERPH_HUMAN	SERPINH1	Serpin H1	0.44	0.17	-1.18	-2.57	-0.89	-2.02
SH3B4_HUMAN	SH3BP4	SH3 domain-binding protein 4	0.11	0.08	-3.15	-3.68	-2.49	-2.92
SNX18_HUMAN	SNX18	Sorting nexin-18	0.05	1.04	-4.41	0.06	-3.51	0.11
SNX3_HUMAN	SNX3	Sorting nexin-3	0.09	0.27	-3.48	-1.91	-2.76	-1.49
STC2_HUMAN	STC2	Stanniocalcin-2	0.24	0.17	-2.04	-2.54	-1.59	-2.00
SYCM_HUMAN	CARS2	Probable cysteine—tRNA ligase, mitochondrial	0.25	0.14	-1.98	-2.82	-1.54	-2.22
TGM2_HUMAN	TGM2	Protein-glutamine gamma-glutamyltransferase 2	0.32	0.07	-1.66	-3.79	-1.29	-3.01
TPM1_HUMAN	TPM1	Tropomyosin alpha-1 chain	0.06	0.15	-4.05	-2.74	-3.21	-2.16
UAP1L_HUMAN	UAP1L1	UDP-N-acetylhexosamine pyrophosphorylase-like protein 1	0.15	0.19	-2.76	-2.42	-2.17	-1.90
UBA6_HUMAN	UBA6	Ubiquitin-like modifier-activating enzyme 6	0.17	0.22	-2.58	-2.20	-2.03	-1.72
UBA7_HUMAN	UBA7	Ubiquitin-like modifier-activating enzyme 7	0.15	0.08	-2.72	-3.66	-2.14	-2.90
UN13D_HUMAN	UNC13D	Protein unc-13 homolog D	0.39	0.10	-1.38	-3.36	-1.05	-2.66
VAT1_HUMAN	VAT1	Synaptic vesicle membrane protein VAT-1 homolog	0.16	0.21	-2.63	-2.25	-2.07	-1.76
VIME_HUMAN	VIM	Vimentin	0.15	0.38	-2.75	-1.40	-2.17	-1.07
WDFY1_HUMAN	WDFY1	WD repeat and FYVE domain-containing protein 1	0.08	0.30	-3.60	-1.72	-2.85	-1.33
WIPI1_HUMAN	WIPI1	WD repeat domain phosphoinositide-interacting protein 1	0.18	0.13	-2.50	-2.97	-1.96	-2.35

[a]Proteins shown have at least one z-score value (M/L or H/L) $\geq$1.960σ in two biological replicates.

doi:10.1371/journal.pone.0134727.t003

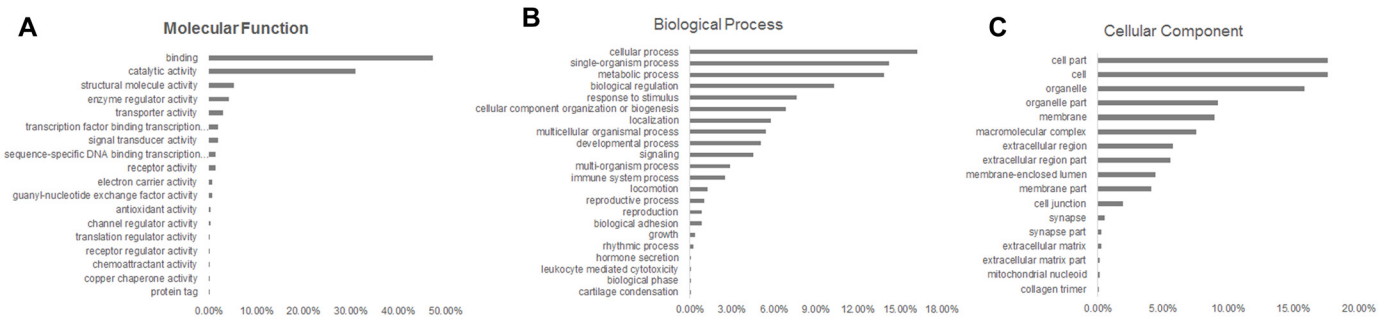

Fig 4. Functional classification of identified proteins using SWISS-PROT database based on universal GO annotation terms. Proteins shown were linked to at least one annotation term within the GO molecular function (A), biological process (B), and cellular component (C) categories.

doi:10.1371/journal.pone.0134727.g004

Confirmation of SILAC and western blotting results by cell staining with antibodies

Antibodies recognizing MAGEA4, THY1, IGF2BP1, VIM, CTNNB1, and FN1 proteins, whose expression differed significantly in BC cells vs. HCV29 cells, were used to confirm the results of previous analyses and to assess protein distributions. Fluorescence signal intensities in the two BC cell lines were significantly higher for MAGEA4, THY1, and IGF2BP1 and significantly lower for VIM, CTNNB1, and FN1, in agreement with SILAC, western blotting, and RT-PCR results. Preferential localization was observed for MAGEA4 in central cytoplasm (including mitochondria and centrosome) and the nuclear region, for THY1 and VIM in cytoplasmic membrane and cytoplasm, for IGF2BP1 in the nuclear region and cytoplasm, and for CTNNB1 and FN1 in cytoplasmic membrane (Fig 7).

Discussion

Urothelial carcinoma of the bladder is unique among epithelial carcinomas in its divergent pathways of tumorigenesis. At the time of diagnosis for transitional cell BC, ~80% of patients are in the low-grade (grade 1–2) non-muscle invasive (cTa or cT1) stage. In patients with low grade Ta disease, the 15-year progression-free survival is 95% with no cancer-specific mortality [36]. Therefore, biomarkers are needed for predicting a risk of stage progression from non-invasive to invasive, or non-metastatic to metastatic and predicting responsiveness to systemic therapies. The human cell lines HCV29 (normal bladder epithelia), KK47 (low grade nonmuscle invasive bladder cancer), and YTS1 (metastatic bladder cancer) have been widely used in studies of molecular mechanisms and cell signaling during the progression of bladder cancer to muscle or metastatic states [37]. However, little attention has been paid to global quantitative proteome analysis of these three cell lines.

Quantitative analysis of proteins at different stages of BC progression is a challenging but important task for understanding of disease mechanisms. SILAC, a differential isotope labeling strategy that involves metabolic labeling of proteins *in vivo*, has been widely applied in cell biology and studies of model organisms such as yeast, bacteria, nematodes, plants, and mice [38, 39]. In SILAC, natural "light" isotopes of carbon, nitrogen, and hydrogen in amino acids incorporated during protein translation are substituted with "heavy" isotopes such as ^{13}C, ^{15}N, and ^{2}H. No study to date has quantified differences in protein abundance at various stages of BC. Previous studies have focused on comparative protein levels in BC patients vs. control subjects, but not on alterations of protein levels during BC progression [8,9].

Identification and characterization of protein levels at various steps of differentiation are essential for our understanding of normal tissue development and malignant transformation.

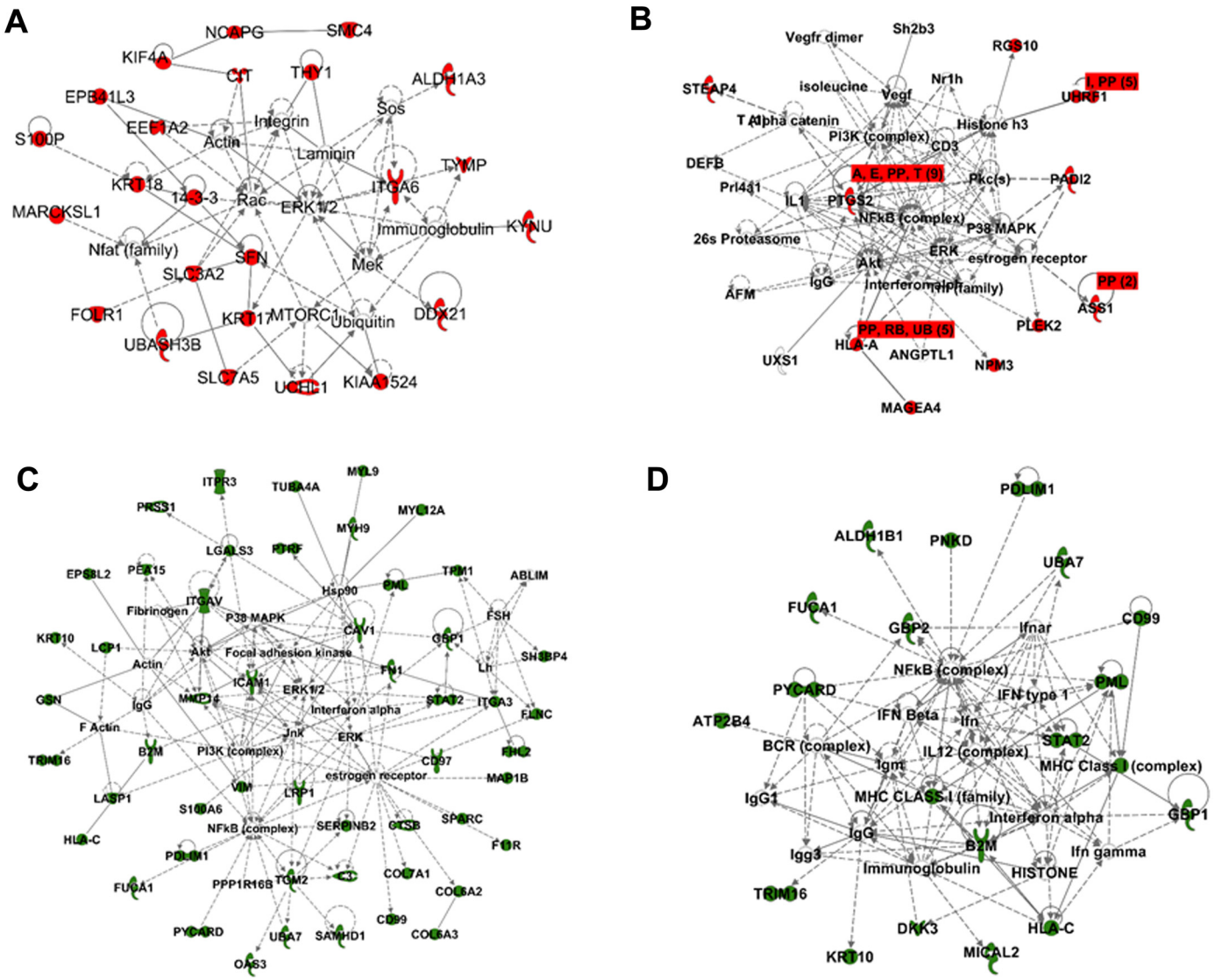

Fig 5. Functional network analysis of differentially regulated proteins with z-score cutoff 95% observed in different stages of BC cells using Ingenuity Pathways Analysis (IPA). (A and B) Top network functions of DNA replication, molecular transport, cell growth, and cell proliferation for upregulated proteins. (C and D) Top network functions of cellular movement, immune cell trafficking, and lipid metabolism. Solid lines: direct known interactions. Dashed lines: suspected or indirect interactions. White: proteins known to be in the network but not identified in our study.

doi:10.1371/journal.pone.0134727.g005

In the present study, we applied the SILAC method to analysis of HCV29, KK47, and YTS1. This strategy provided protein information for all three cell lines during one MS experiment. Following normalization by the z-score method, differential regulation was observed for 110 proteins in KK47 vs. HCV29 and for 87 proteins in YTS1 vs. HCV29. These differentially regulated proteins, which may play important roles in BC development, include SFN (14-3-3 protein sigma), SELENBP1 (selenium-binding protein 1), COL6A3 (collagen α3 (VI) chain), and CD70. COL6A2 and COL6A3 protein levels are reduced in urine of BC patients [40]. SFN is downregulated in invasive bladder transitional cell carcinomas undergoing epithelial-to-mesenchymal conversion and highly upregulated in pure squamous cell carcinomas [41]. Some of the proteins that are altered in BC are also altered in other cancers. In particular, expression of FOLR1 (folate receptor alpha) is increased relative to normal tissue in many types of epithelial

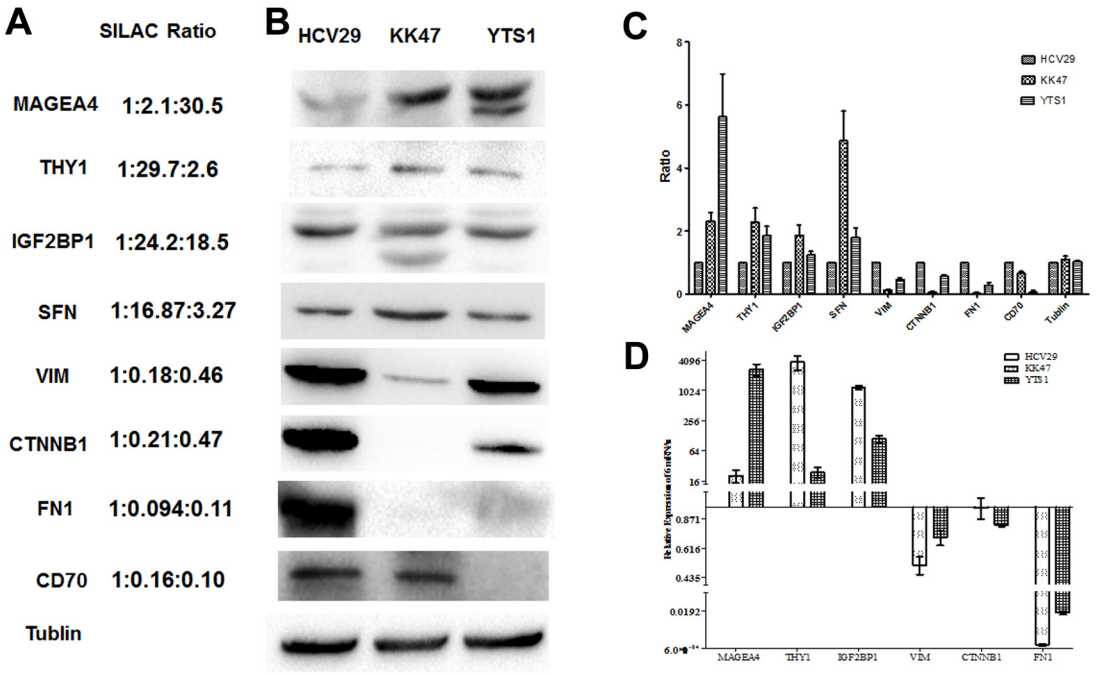

Fig 6. Confirmation of SILAC-determined protein and RNA abundances. (A) SILAC L:M:H average ratios for six selected proteins. (B) Western blotting analysis of selected proteins. Proteins were transferred to a PVDF membrane, probed with their primary antibodies, and incubated with HRP-conjugated rabbit anti-mouse or goat anti-rabbit secondary antibodies. (C) Densitometric quantitation of the protein levels. The protein was normalized by the tublin, and then compared to HCV29, which were arbitrarily set at 1.0. (D) Gene expression for the proteins was analyzed by qRT-PCR. Relative expression in comparison to control samples was analyzed by the $2^{-\Delta\Delta Ct}$ method and represented as Log_2. Expression of genes above $Log_2(2)$ or below $Log_2(1/2)$ was significantly upregulated or downregulated, respectively.

doi:10.1371/journal.pone.0134727.g006

cancer, including non-mucinous ovarian, endometrial, non-small cell lung, colorectal, and breast cancers [42].

The DAVID bioinformatic resources provide a set of powerful tools to explore their large gene lists in depth from many different biological perspectives in order to fully extract associated biological meanings. Enrichment analysis of GO terms in our identified proteins indicated that neutral amino acid transmembrane transporter activity and metabolic processes were significantly upregulated and that protein binding, cell adhesion, biological adhesion, and immune response were significantly downregulated in the BC cell lines. The observed changes in GO terms tended to promote cellular proliferation, tumor development, cancer cell progression and metastasis, and escape from immune system surveillance.

A major challenge in cancer biology is the formulation of biological hypotheses regarding biomarker candidates [43]. Pathway analysis of differentially expressed proteins indicates that DNA replication and molecular transport, cell growth, and cell proliferation are requirements for cancer cell metastasis. Intercellular adhesion molecule-1 (iCAM-1) is a transmembrane glycoprotein present at basal levels in a wide variety of cell types and is upregulated in response to a number of inflammatory mediators [44]. The biological significance of iCAM-1 expression in cancer remains controversial; it is elevated in gastric, breast, oral, and thyroid cancer tissues [44–47] but reduced in some ovarian adenocarcinoma cell lines and primary tumors [48]. Also, iCAM-1 expression is up-regulated in squamous cell types associated with inflammation, such as schistosomal bladder cancer [49]. However, in the present study, iCAM-1 expression was reduced in metastatic bladder cancer cells. Moreover, CIT, a novel tissue-specific Ser/Thr kinase that encompasses the Rho-Rac-binding protein Citron, plays a role in cytokinesis and in

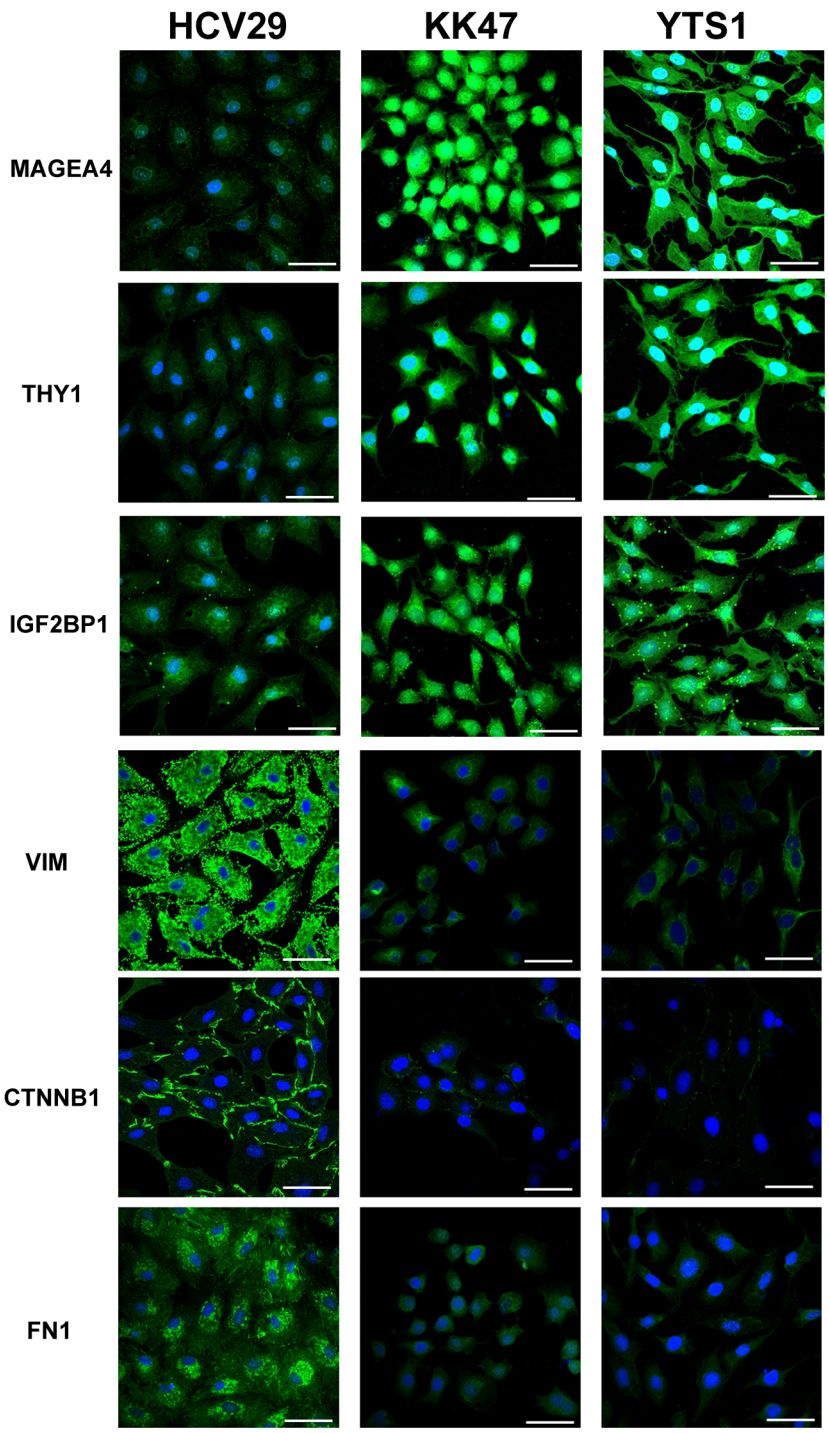

Fig 7. Differential expression revealed by cell staining. HCV29, KK47, and YTS1 cells were cultured and stained with six antibodies directed to identified proteins (MAGEA4, THY1, IGF2BP1, VIM, CTNNB1, FN1) labeled with Cy3 as described in M&M. Images are shown of merge images of Cy3-conjugated antibodies and DAPI staining of nuclei (objective magnification 60×). Scale bars: 70 μm.

doi:10.1371/journal.pone.0134727.g007

Rho signaling that modulates myosin phosphorylation and cell adhesion [50]. Upregulation of CIT promotes DNA replication and cancer cell proliferation.

In conclusion, we successfully applied the SILAC method to identify and quantify proteins whose level is significantly up- or downregulated during BC development or progression. Similar advanced proteome techniques will be useful for further elucidation of biomarkers and molecular mechanisms in BC and other types of cancer.

Supporting Information

S1 Fig. Protein raw ion intensities for western blot.
(TIF)

S1 Table. The full list of proteins identified by 2D-LC-MS/MS.
(XLSX)

S2 Table. Gene ontology statistics of significantly upregulated and downregulated proteins.
(XLSX)

Acknowledgments

The authors are grateful to Dr. S. Anderson for English editing of the manuscript.

Author Contributions

Conceived and designed the experiments: FG GLY PX. Performed the experiments: GLY WL JG CWS ZPX. Analyzed the data: GLY XL ZPX. Contributed reagents/materials/analysis tools: GLY WL. Wrote the paper: GLY FG.

References

1. Siegel R, Ma J, Zou Z, Jemal A (2014) Cancer statistics, 2014. CA Cancer J Clin 64: 9–29. doi: 10.3322/caac.21208 PMID: 24399786
2. Wang H, Cai Z, Yang F, Luo J, Satoh M, Arai Y, et al. (2014) Enhanced antitumor efficacy of integrin-targeted oncolytic adenovirus AxdAdB3-F/RGD on bladder cancer. Urology 83: 508 e513–509.
3. Goodison S, Rosser CJ, Urquidi aV (2009) Urinary proteomic profiling for diagnostic bladder cancer biomarkers. Expert Rev Proteomics 6: 507–514. doi: 10.1586/epr.09.70 PMID: 19811072
4. Wu XR (2005) Urothelial tumorigenesis: a tale of divergent pathways. Nature Reviews Cancer 5: 713–725. PMID: 16110317
5. Volkmer J-P, Sahoo D, Chin RK, Ho PL, Tang C, Kurtova AV, et al. (2012) Three differentiation states risk-stratify bladder cancer into distinct subtypes. Proc Natl Acad Sci U S A 109: 2078–2083. doi: 10.1073/pnas.1120605109 PMID: 22308455
6. Weissman I (2005) Stem Cell Research: Paths to Cancer Therapies and Regenerative Medicine. J Am Med Assoc 294: 1359–1366.
7. Available: http://www.cancer.org/acs/groups/cid/documents/webcontent/003085-pdf.pdf. Accessed 23 June 2015.
8. Linden M, Lind SB, Mayrhofer C, Segersten U, Wester K, Lyutvinskiy Y, et al. (2012) Proteomic analysis of urinary biomarker candidates for nonmuscle invasive bladder cancer. Proteomics 12: 135–144. doi: 10.1002/pmic.201000810 PMID: 22065568
9. Kreunin P, Zhao J, Rosser C, Urquidi V, Lubman DM, Goodison S (2007) Bladder Cancer Associated Glycoprotein Signatures Revealed by Urinary Proteomic Profiling. J Proteome Res 6: 2631–2639. PMID: 17518487
10. Cheng L, Davison DD, Adams J, Lopez-Beltran A, Wang L, Montironi R, et al. (2014) Biomarkers in bladder cancer: translational and clinical implications. Crit Rev Oncol Hematol 89: 73–111. doi: 10.1016/j.critrevonc.2013.08.008 PMID: 24029603

11. Goodison S, Rosser CJ, Urquidi V (2013) Bladder cancer detection and monitoring: assessment of urine- and blood-based marker tests. Mol Diagn Ther 17: 71–84. doi: 10.1007/s40291-013-0023-x PMID: 23479428
12. Tian Y, Bova GS, Zhang H (2011) Quantitative glycoproteomic analysis of optimal cutting temperature-embedded frozen tissues identifying glycoproteins associated with aggressive prostate cancer. Anal Chem 83: 7013–7019. doi: 10.1021/ac200815q PMID: 21780747
13. Rong Y, Jin D, Hou C, Hu J, Wu W, Ni X, et al. (2010) Proteomics analysis of serum protein profiling in pancreatic cancer patients by DIGE: up-regulation of mannose-binding lectin 2 and myosin light chain kinase 2. BMC Gastroenterol 10: 68. doi: 10.1186/1471-230X-10-68 PMID: 20587030
14. Chen J-S, Chen K-T, Fan C-W, Han C-L, Chen Y-J, Yu J-S, et al. (2010) Comparison of membrane fraction proteomic profiles of normal and cancerous human colorectal tissues with gel-assisted digestion and iTRAQ labeling mass spectrometry. FEBS J 277: 3028–3038. doi: 10.1111/j.1742-4658.2010.07712.x PMID: 20546304
15. Caceres NE, Aerts M, Marquez B, Mingeot-Leclercq MP, Tulkens PM, Devreese B, et al. (2013) Analysis of the membrane proteome of ciprofloxacin-resistant macrophages by stable isotope labeling with amino acids in cell culture (SILAC). PLoS One 8: e58285. doi: 10.1371/journal.pone.0058285 PMID: 23505477
16. Ong S-E, Blagoev B, Kratchmarova I, Kristensen DB, Steen H, Pandey A, et al. (2002) Stable isotope labeling by amino acids in cell culture, SILAC, as a simple and accurate approach to expression proteomics. Mol Cell Proteomics 1: 376–386. PMID: 12118079
17. Ahmad Y, Lamond AI (2014) A perspective on proteomics in cell biology. Trends Cell Biol 24: 257–264. doi: 10.1016/j.tcb.2013.10.010 PMID: 24284280
18. Masters JRW, Hepburn PJ, Walker L, Highman WJ, Trejdosiewicz LK, Povey S, et al. (1986) Tissue Culture Model of Transitional Cell Carcinoma_ Characterization of Twenty-two Human Urothelial Cell Lines. Cancer Res 46: 3630–3637. PMID: 3708594
19. Hisazumi H, Kanokogi M, Nakajima K, Kobayashi T, Tsukahara K, Naito K, et al. (1979) Established cell line of urinary bladder carcinoma (KK-47): growth, heterotransplantation, microscopic structure and chromosome pattern. Jpn J Urol 70: 485–494.
20. Kakizaki H, Numasawa K, Suzuki K (1986) Establishment of a new cell line (YTS-1) derived from a human urinary bladder carcinoma and its characteristics. Jpn J Urol 77: 1790–1795.
21. Bendall SC, Hughes C, Stewart MH, Doble B, Bhatia M, Lajoie GA (2008) Prevention of amino acid conversion in SILAC experiments with embryonic stem cells. Mol Cell Proteomics 7: 1587–1597. doi: 10.1074/mcp.M800113-MCP200 PMID: 18487603
22. Takakura D, Hashii N, Kawasaki N (2013) An improved in-gel digestion method for efficient identification of protein and glycosylation analysis of glycoproteins using guanidine hydrochloride. Proteomics 14:196–201.
23. Yang G, Cui T, Wang Y, Sun S, Ma T, Wang T, et al. (2013) Selective isolation and analysis of glycoprotein fractions and their glycomes from hepatocellular carcinoma sera. Proteomics 13: 1481–1498. doi: 10.1002/pmic.201200259 PMID: 23436760
24. Washburn MP, Wolters D, Yates JR III (2001) Large-scale analysis of the yeast proteome by multidimensional protein identification technology. Nat Biotechnol 19: 242–247. PMID: 11231557
25. Hong Q, Xue P, Liu S, Bo F, Yang L, Huang Z, et al. (2011) Differentially Expressed Protein Profile of Renal Tubule Cell Stimulated by Elevated Uric Acid Using SILAC Coupled to LC-MS. Cell Physiol Biochem 27: 91–98. doi: 10.1159/000325209 PMID: 21325826
26. Cox J, Mann M (2008) MaxQuant enables high peptide identification rates, individualized p.p.b.-range mass accuracies and proteome-wide protein quantification. Nat Biotechnol 26: 1367–1372. doi: 10.1038/nbt.1511 PMID: 19029910
27. Cox J, Matic I, Hilger M, Nagaraj N, Selbach M, Olsen JV, et al. (2009) A practical guide to the MaxQuant computational platform for SILAC-based quantitative proteomics. Nature Protocols 4: 698–705. doi: 10.1038/nprot.2009.36 PMID: 19373234
28. Cox J, Neuhauser N, Michalski A, Scheltema RA, Olsen JV, Mann M (2011) Andromeda: a peptide search engine integrated into the MaxQuant environment. J Proteome Res 10: 1794–1805. doi: 10.1021/pr101065j PMID: 21254760
29. Berard AR, Cortens JP, Krokhin O, Wilkins JA, Severini A, Coombs KM (2012) Quantification of the Host Response Proteome after Mammalian Reovirus T1L Infection. PLoS One 7: e51939. doi: 10.1371/journal.pone.0051939 PMID: 23240068
30. Coombs KM, Berard A, Xu W, Krokhin O, Meng X, Cortens JP, et al. (2010) Quantitative proteomic analyses of influenza virus-infected cultured human lung cells. J Virol 84: 10888–10906. doi: 10.1128/JVI.00431-10 PMID: 20702633

31. Camon E, Magrane M, Barrell D, Binns D, Fleischmann W, Kersey P, et al. (2003) The Gene Ontology Annotation (GOA) project: implementation of GO in SWISS-PROT, TrEMBL, and InterPro. Genome Res 13: 662–672. PMID: 12654719

32. Huang DW, Sherman BT, Tan Q, Kir J, Liu D, Bryant D, et al. (2007) DAVID Bioinformatics Resources: expanded annotation database and novel algorithms to better extract biology from large gene lists. Nucleic Acids Res 35: W169–W175. PMID: 17576678

33. Huang DW, Sherman BT, Lempicki RA (2009) Systematic and integrative analysis of large gene lists using DAVID bioinformatics resources. Nat Protoc 4: 44–57. doi: 10.1038/nprot.2008.211 PMID: 19131956

34. Yang G, Chu W, Zhang H, Sun X, Cai T, Dang L, et al. (2013) Isolation and identification of mannose-binding proteins and estimation of their abundance in sera from hepatocellular carcinoma patients. Proteomics 13: 878–892. doi: 10.1002/pmic.201200018 PMID: 23300094

35. Livak KJ, Schmittgen TD (2001) Analysis of Relative Gene Expression Data Using Real-Time Quantitative PCR and the $2^{<-\Delta\Delta CT>}$ Method. Methods 25: 402–408. PMID: 11846609

36. Kaufman DS, Shipley WU, Feldman AS (2009) Bladder cancer. Lancet 375: 239–249.

37. Yang G, Tan Z, Lu W, Guo J, Yu H, Yu J, et al. (2015) Quantitative glycome analysis of N-glycan patterns in bladder cancer vs normal bladder cells using an integrated strategy. J Proteome Res 14: 639–653. doi: 10.1021/pr5006026 PMID: 25536294

38. Matic I, Jaffray EG, Oxenham SK, Groves MJ, Barratt CL, Tauro S, et al. (2011) Absolute SILAC-compatible expression strain allows Sumo-2 copy number determination in clinical samples. J Proteome Res 10: 4869–4875. doi: 10.1021/pr2004715 PMID: 21830832

39. Kruger M, Moser M, Ussar S, Thievessen I, Luber CA, Forner F, et al. (2008) SILAC mouse for quantitative proteomics uncovers kindlin-3 as an essential factor for red blood cell function. Cell 134: 353–364. doi: 10.1016/j.cell.2008.05.033 PMID: 18662549

40. Lei T, Zhao X, Jin S, Meng Q, Zhou H, Zhang M (2013) Discovery of potential bladder cancer biomarkers by comparative urine proteomics and analysis. Clin Genitourin Cancer 11: 56–62. doi: 10.1016/j.clgc.2012.06.003 PMID: 22982111

41. Moreira JM, Gromov P, Celis JE (2004) Expression of the tumor suppressor protein 14-3-3 sigma is down-regulated in invasive transitional cell carcinomas of the urinary bladder undergoing epithelial-to-mesenchymal transition. Mol Cell Proteomic 3: 410–419.

42. Despierre E, Lambrechts S, Leunen K, Berteloot P, Neven P, Amant F, et al. (2013) Folate receptor alpha (FRA) expression remains unchanged in epithelial ovarian and endometrial cancer after chemotherapy. Gynecol Oncol 130: 192–199. doi: 10.1016/j.ygyno.2013.03.024 PMID: 23558051

43. Lawlor K, Nazarian A, Lacomis L, Tempst P, Villanueva J (2009) Pathway-Based Biomarker Search by High-Throughput Proteomics Profiling of Secretomes. J Proteome Res 8: 1489–1503. doi: 10.1021/pr8008572 PMID: 19199430

44. Usami Y, Ishida K, Sato S, Kishino M, Kiryu M, Ogawa Y, et al. (2013) Intercellular adhesion molecule-1 (ICAM-1) expression correlates with oral cancer progression and induces macrophage/cancer cell adhesion. Int J Cancer 133: 568–578. doi: 10.1002/ijc.28066 PMID: 23364881

45. Maruo Y, Gochi A, Kaihara A, Shimamura H, Yamada T, Tanaka N, et al. (2002) ICAM-1 expression and the soluble ICAM-1 level for evaluating the metastatic potential of gastric cancer. Int J Cancer 100: 486–490. PMID: 12115535

46. Schroder C, Witzel I, Muller V, Krenkel S, Wirtz RM, Janicke F, et al. (2011) Prognostic value of intercellular adhesion molecule (ICAM)-1 expression in breast cancer. J Cancer Res Clin Oncol 137: 1193–1201. doi: 10.1007/s00432-011-0984-2 PMID: 21590495

47. Buitrago D, Keutgen XM, Crowley M, Filicori F, Aldailami H, Hoda R, et al. (2012) Intercellular adhesion molecule-1 (ICAM-1) is upregulated in aggressive papillary thyroid carcinoma. Ann Surg Oncol 19: 973–980. doi: 10.1245/s10434-011-2029-0 PMID: 21879273

48. Arnold J, Cummings M, Purdie D, Chenevix-Trench G (2001) Reduced expression of intercellular adhesion molecule-1 in ovarian adenocarcinomas. Br J Cancer 85: 1351–1358. PMID: 11720474

49. Khaled H (2013) Schistosomiasis and cancer in egypt: review. J Adv Res 4: 461–466. doi: 10.1016/j.jare.2013.06.007 PMID: 25685453

50. Schwartz M (2004) Rho signalling at a glance. J Cell Sci 117: 5457–5458. PMID: 15509861